IV. Conclusions

Two original electronically switchable microstrip-line directional filters are presented. They provide substantially improved frequency characteristics compared to the conventional constructions. The unique feature of them is that they offer high-level isolation, independent of frequency, over a wide frequency range for two pairs of opposite ports. These isolation characteristics are also independent of the p-i-n diode parameters if the diodes used are identical. It should be pointed out that the above conclusions relate to the filters operating in two modes (reception and transmission), i.e., when the diodes are forward or reverse biased. Thus, these directional filters seem to be suitable for some radio-communication applications.

Appendix

Fig. 10 presents equivalent circuits for MA4P7000 p-i-n diode under forward and reverse bias. The following parameters have been used for calculations: $C_p = 0.001$ pF, $L_p = 0.001$ nH, $R_s(I_0 = 100\ \text{mA}) = 0.8\ \Omega$, $C_T(U_R = 100\ \text{V}) = 0.70$ pF, and $R(U_R = 100\ \text{V}) = 200\ k\Omega$.

References

[1] S. B. Cohn and F. S. Coale, "Directional channel separation filters," *Proc. IRE*, vol. 44, pp. 1018–1024, Aug. 1956.

[2] R. D. Wanselow and L. P. Tuttle, Jr., "Practical design of strip transmission line half-wavelength resonator directional filters," *IRE Trans. Microwave Theory Tech.*, vol. MTT-7, pp. 168–173, Jan. 1959.

[3] G. L. Matthaei, L. Young, and E. M. T. Jones, *Microwave Filters, Impedance Matching Networks and Coupling Structures.* New York: McGraw-Hill, 1964, ch. 14.

[4] T. Q. Ho and S. M. Hart, "A broad-band coplanar waveguide to slotline transition," *IEEE Microwave Guided Wave Lett.*, vol. 2, pp. 415–416, Oct. 1992.

[5] V. F. Fusco and Q. Chen, "Slotline short and open circuit analysis by the finite-difference time-domain method," in *Proc. 24th European Microwave Conf.*, vol. 2, Cannes, France, 1994, pp. 1720–1726.

[6] J. Reed and G. Wheeler, "A method of analysis of symmetrical four-port networks," *IRE Trans. Microwave Theory Tech.*, vol. MTT-4, pp. 246–252, Oct. 1956.

[7] S. Rosloniec and P. Lochowicz, "Split-tee power divider," *RF Design*, vol. 13, pp. 65–69, Sept. 1990.

[8] M. W. Medley, Jr., *Microwave and RF Circuits, Analysis, Synthesis and Design.* Norwood, MA: Artech House, 1993.

[9] R. W. Anderson, "S-parameter techniques for faster, more accurate network design," *Hewlett-Packard J.*, vol. 18, no. 6, pp. 13–24, Feb. 1967. [This paper is also reprinted in Hewlett-Packard Appl. Note 95-1.]

[10] M/A COM Catalogue, *RF and Microwave Semiconductors*. Burlington, MA, pp. 19–24, 1994.

Radiation Properties of a Planar Dielectric Waveguide Loaded with Conducting-Strip Diffraction Grating

Aleksander Błędowski and Władysław Żakowicz

***Abstract*—A dielectric planar waveguide periodically loaded with conducting strips is considered as a possible antenna for millimeter-wave range. We show that separating the grating from the waveguide leads to the reduction of radiative attenuation of the waveguided radiation and substantial narrowing of the angular spread of the diffracted radiation.**

***Index Terms*—Diffraction grating antennas, leaky-wave antennas.**

I. Introduction

Diffraction gratings placed on the surface of dielectric waveguides are very important components of many microwave devices serving either as transmitting or receiving antennas and also subject to numerous theoretical and experimental studies.

Our theoretical analysis, developed along a general electromagnetic theory of gratings [1] and [2], is devoted to a planar dielectric waveguide loaded with periodic infinitely thin metallic strips made of perfect conductor. We consider this system for a millimeter-wavelength radiation.

Similar systems have often been studied in the past in [3]–[6]. Generalizing these discussions, we admit an additional gap between the grating and the waveguide, allowing better control of the coupling between the guided and diffracted waves. For a weaker coupling and correspondingly slower attenuation, the outgoing beam can be concentrated in a much narrower angular sector. Often this is a desired beam property. Such a grating separation is present in a technical construction of a millimeter-wave antenna with variable grating period [8].

In Section II, the basic equations describing waves in the investigated structure are derived. We consider only the waves propagating perpendicularly to the strips and having either TE or TM polarizations. In Section III, numerical results showing the complex propagation constant as a function of the various waveguide and grating parameters are presented. Some discussion on the angular width of the diffracted radiation is also given.

II. Theory

We consider a dielectric waveguide of thickness h and dielectric constant ϵ_w loaded with a diffraction grating formed by parallel metallic strips distributed periodically with a period d. The grating is separated from the waveguide by a dielectric layer of thickness b and dielectric constant ϵ_b. The metallic strips are made of perfect conductor, have width w, and infinitesimal thickness. The whole system is surrounded by a homogeneous dielectric medium with dielectric constant ϵ_v. The system, along with a coordinate system used, are shown in Fig. 1.

We assume the electromagnetic waves to be monochromatic with the time-dependence factor $\exp(i\omega t)$, perpendicularly propagating

Manuscript received June 26, 1996; revised May 19, 1997. This paper was supported in part by the Physical Optics Corporation (POC), Torrance, CA.

The authors are with the Institute of Physics, Polish Academy of Sciences, Warsaw 02-668, Poland.

Publisher Item Identifier S 0018-9480(97)06069-9.

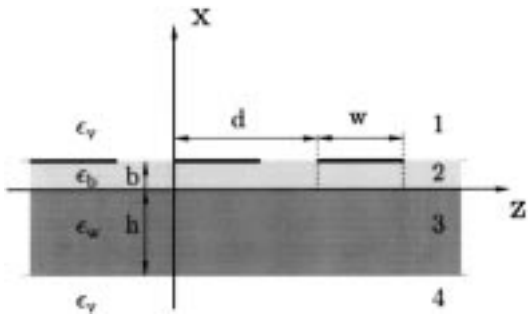

Fig. 1. Geometry of the dielectric waveguide with metallic diffraction grating. Regions 1 and 4 correspond to a cover vacuum, region 3 to the waveguide, and region 2 to the spacing dielectric layer.

to the grating strips, i.e., along the z-axis. Thus, the waves are y-independent and can be attributed to two polarization classes called TE and TM polarization. In both polarizations, the relevant component of the EM field satisfies the same equation:

$$\phi_{xx} + \phi_{zz} + k_o^2 \epsilon(x)\phi = 0 \tag{1}$$

where $\phi(x,z)$ stands for $E_y(x,z)$ in the TE case, and for $H_y(x,z)$ in the TM case. $\epsilon(x)$ is equal to ϵ_v, ϵ_b, or ϵ_w, depending on the layer, and $k_o = \omega/c$. According to Maxwell equations, the remaining field components (H_x and H_z in the TE case and E_x and E_z in the TM case) can be obtained from ϕ by differentiation.

Due to the periodicity of the system, we can make use of the Floquet theorem and look for solutions in the form of quasi-periodic functions. For both polarizations, the function $\phi(x,z)$ in four regions $1'$, $2'$, $3'$, and $4'$ (shown in Fig. 1) can be assumed in the following form:

$$\phi(x,z) = \sum_{n=-\infty}^{\infty} \exp(-i\beta_n z) \times \begin{cases} a_n \exp[-iq_n^v(x-b)], & (1') \\ b_n \cos q_n^b x + c_n \sin q_n^b x, & (2') \\ d_n \cos q_n^w x + e_n \sin q_n^w x, & (3') \\ f_n \exp[iq_n^v(x+h)], & (4'). \end{cases} \tag{2}$$

The particular form of the x-dependence comes from (1). The coefficients β_n, q_n, etc., are $\beta_n = \beta_o + nK = \beta_o + n(2\pi/d)$, $q_n^v = \sqrt{\epsilon_v k_o^2 - \beta_n^2}$, $q_n^w = \sqrt{\epsilon_w k_o^2 - \beta_n^2}$, and $q_n^b = \sqrt{\epsilon_b k_o^2 - \beta_n^2}$, with β_o being the complex free parameter to be determined. A proper branch selection of the multivalued square-root function above is discussed in [2].

The amplitudes $a_n, \cdots, f_n$ in (2) must be chosen in such a way that the field-continuity conditions are fulfilled. The homogeneity of interfaces between regions $2'$–$3'$ and $3'$–$4'$ ensures that the relationships between b_n, c_n, d_n, e_n, and f_n can be determined analytically. For TE polarization

$$\begin{aligned} d_n &= \left(\cos q_n^w h + i\frac{q_n^v}{q_n^w}\sin q_n^w h\right) f_n \\ e_n &= \left(-\sin q_n^w h + i\frac{q_n^v}{q_n^w}\cos q_n^w h\right) f_n \\ b_n &= d_n, \quad c_n = \frac{q_n^w}{q_n^b} e_n. \end{aligned} \tag{3}$$

In the corresponding expressions for TM polarization, one must replace

$$\frac{q_n^v}{q_n^w} \to \frac{q_n^v \epsilon_w}{q_n^w \epsilon_v} \quad \text{and} \quad \frac{q_n^w}{q_n^b} \to \frac{q_n^w \epsilon_b}{q_n^b \epsilon_w}. \tag{4}$$

The tangent-field values just beneath the grating are

$$\begin{aligned} \phi(x = b^-, z) &= \sum e^{-i\beta_n z}[b_n \cos q_n^b b + c_n \sin q^b b] \\ &= \sum e^{-i\beta_n z} p_n f_n, \\ \phi_{,x}(x = b^-, z) &= \sum e^{-i\beta_n z} q_n^b [-b_n \sin q_n^b b + c_n \cos q^b b] \\ &= \sum e^{-i\beta_n z} q_n^b r_n f_n. \end{aligned} \tag{5}$$

At the interface occupied by the grating, one has the continuity conditions between the grating strips, as well as the boundary conditions at the top and bottom sides of the conductors.

For the TE waves, the continuity of E_y and H_z in the interval $0 \le z < d - w$ leads to

$$\begin{aligned} \sum a_n \exp(-i\beta_n z) - \sum f_n p_n \exp(-i\beta_n z) = 0 \\ \sum a_n (-iq_n^v) \exp(-i\beta_n z) - \sum f_n q_n^b r_n \exp(-i\beta_n z) = 0 \end{aligned} \tag{6}$$

while for $d - w \le z < d$, the condition $E_y = 0$ on both strip sides gives

$$\begin{aligned} \sum a_n \exp(-i\beta_n z) + 0 = 0 \\ 0 + \sum f_n p_n \exp(-i\beta_n z) = 0. \end{aligned} \tag{7}$$

The corresponding equations for the TM polarization are very similar.

Equations (6) and (7) taken at each value of z form an infinite set of linear homogeneous equations for two countable and infinite sets of amplitudes a_n and f_n. The numerical approach used in this paper utilizes truncation of this set to a finite number of amplitudes as well as a discretization of the z-variable at the equally spaced points z_n. A consistency of this procedure to the Nth order is guaranteed, if we select $2(2N+1)$ amplitudes $a_{-N}, \cdots, a_N$ and $f_{-N}, \cdots, f_N$ and than we impose the continuity/boundary conditions at the $2N+1$ points $z_m = (m - 0.5)\Delta$, $\Delta = d/(2N+1)$, $m = 1, \cdots, 2N+1$. In this way, the problem is reduced to the finite and homogeneous set of $2(2N+1)$ linear algebraic equations. It can be written in the matrix form

$$\boldsymbol{M} \cdot \boldsymbol{u} = \boldsymbol{0} \tag{8}$$

where $\boldsymbol{u} = (a_{-N}, \cdots, a_N, f_{-N}, \cdots, f_N)$. The form of the matrix $\boldsymbol{M}$ can be deduced from (6) and (7).

Nonvanishing solutions of this set exist only when

$$\det \boldsymbol{M} = 0. \tag{9}$$

The determinant depends (besides on all geometrical and material parameters) on the value of β_o. With other parameters fixed, (9) gives permitted values of β_o. For each β_o satisfying the characteristic equation, there exists a nontrivial solution of (8) for the $\boldsymbol{u}$ vector.

III. Results

Our numerical examples refer to a planar quartz waveguide ($SiO_2, \epsilon_w = 3.78$) with metallic grating made of perfect conductor. The operating frequency is assumed to be around 90 GHz, so the typical dimensions for wavelengths, waveguide thickness, grating period, and grating separation are in the millimeter range. The surrounding media as well as the layer separating the grating from the waveguide are assumed to be vacuum ($\epsilon_b = \epsilon_v = 1$). The waveguides chosen in our examples are operating in a single-mode regime, so their thickness does not exceeds 1 mm. Under this condition, we have found that several dozens of amplitudes (both a_n and f_n) have to be used in order to reach a reasonable accuracy of the method.

In Fig. 2, the real and imaginary part of β_o for the TE waves as a function of the grating period for two grating separations are

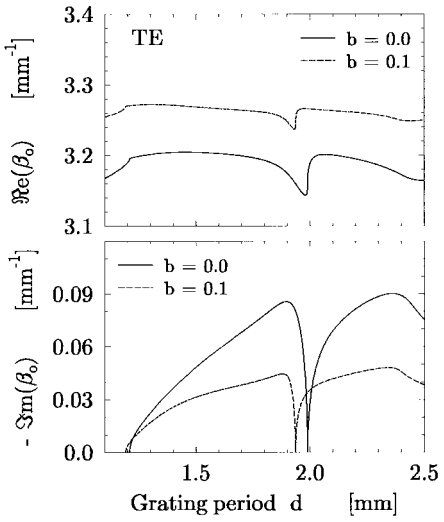

Fig. 2. Propagation constant $\Re e\beta$ and attenuation constant $-\Im m\beta$ as a function of the grating period d. TE case: $k_o = 2\,\text{mm}^{-1}$, $h = 1$ mm, $w/d = 0.5$.

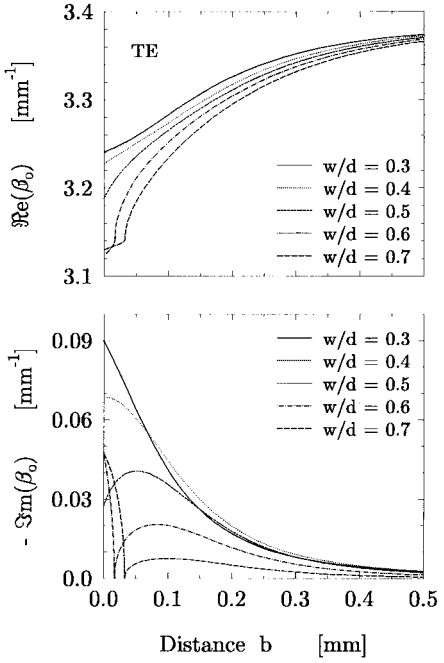

Fig. 3. $\Re e\beta$ and $\Im m\beta$ as a function of the separation distance b for several w/d ratios. TE polarization, thick waveguide: $h = 1$ mm, $k_o = 2\,\text{mm}^{-1}$, $d = 2$ mm.

shown. For small grating periods (d <1.2 mm) there are no diffracted waves. Nonvanishing $\Im m(\beta_o)$ for d >1.2 mm is associated with the existence of diffracted waves and the corresponding energy leakage from the waveguide. The curves behave rather smoothly in this interval—except the vicinity of $d = 2$ mm. Here, the diffracted wave would propagate perpendicularly to the waveguide, but as the damping constant approaches zero this diffraction is absent. Similar phenomena has also been reported in [3].

Separating the grating from the waveguide decreases the phase velocity $v_\phi = \omega/\Re e(\beta_o)$ and the damping. The increase of $\Re e(\beta_o)$ with growing grating separation is a typical property of TE modes. As is seen in the figure, in this strongly bounded-wave case, the separation $b = 0.1$ mm (1/10 of the waveguide thickness) is enough to reduce the damping constant by a factor of two.

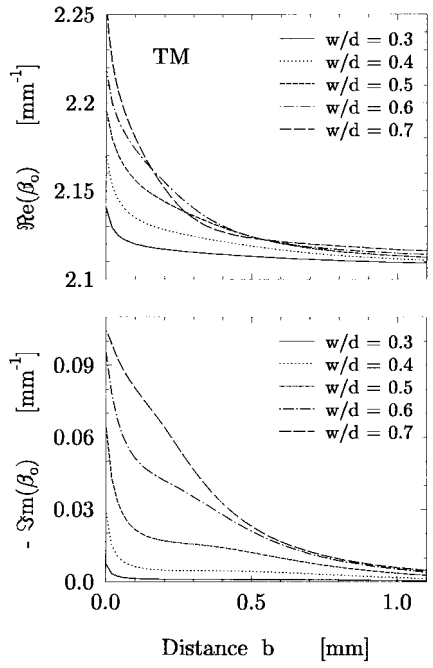

Fig. 4. $\Re e\beta$ and $\Im m\beta$ as a function of the separation distance b for several w/d ratios. TM polarization: $h = 0.4$ mm, $k_o = 2\,\text{mm}^{-1}$, $d = 2$ mm.

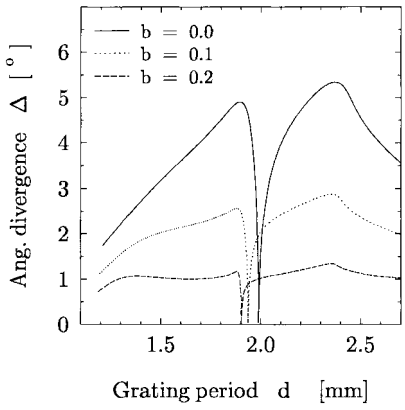

Fig. 5. Angular divergence of the diffracted beam as a function of the grating period d. TE polarization: $h = 1$ mm, $k_o = 2\,\text{mm}^{-1}$, $d = 2$ mm.

In Fig. 3, a dependence of the propagation constant β_o on the grating separation b for several values of the w/d ratio is given. The way the w/d ratio influence β_o is generally complex. However, when one operates away from the regime corresponding to the *perpendicular diffraction* the picture becomes simpler. With increasing w/d ratio, $\Re e(\beta_o)$ gets smaller, while the damping constant first increases and than decreases, typically reaching its maximum at the some value between $w/d = 0.4$ and 0.7. In the thin waveguides, the TE waves can propagate only when the grating separation exceeds some critical distance.

Phase constant and damping constant as functions of the grating separation b for several w/d ratios in the case of TM polarization are shown in Fig. 4. In contrast to the TE case, for this polarization the increase of the grating separation causes the decrease of the phase constant $\Re e(\beta_o)$. Another interesting feature is that the TM diffraction seems to prefer larger values of w/d as opposite to the TE diffraction—the succession of curves in Fig. 4(b) is just reversed, as given in Fig. 3(b). The same effect has been reported in [5].

In Fig. 5, we show the calculated angular divergence of the diffracted beam as the function of grating period d for chosen grating

separations b. Other parameters are the same as in Fig. 2. The curves have been obtained from the far-field angular intensity distribution

$$|\phi(r,\vartheta)|^2 \simeq |a_1|^2 \frac{1}{2\pi kr} \frac{k^2\cos^2\vartheta}{[\Im m(\beta_1)]^2 + [\Re e(\beta_1) - k\sin\vartheta]^2} \quad (10)$$

with the angular divergence Δ defined as the half-width of this distribution. Here, ϑ is an angle between the vector $\boldsymbol{r} = (x, z)$ and the positive x-axis, and $r = |\boldsymbol{r}|$. Equation (10) has been calculated with the help of a appropriate two-dimensional (2-D) diffraction integral [7].

It is seen from Fig. 5 that the value of Δ decreases and becomes a smoother function of d when the grating separation becomes larger. This is a consequence of a weaker coupling of the guided mode with the grating at large separations and smaller changes of the propagation parameters with the varying grating period. Smoothing of the Δ-curves goes together with the narrowing of the radiated beams. It is a fortunate property for applications, where the wide scanning angles and narrow beams are of great importance.

ACKNOWLEDGMENT

The authors acknowledge thanks to the Physical Optics Corporation (POC), Torrance, CA, whose work on millimeter antenna development [8] provided them with motivation. Discussions with R. Gajewski, V. Manasson, and L. Sadovnik of the POC are also gratefully acknowledged.

REFERENCES

[1] R. Petit, Ed., *Electromagnetic Theory of Gratings*. Berlin, Germany: Springer-Verlag, 1980.
[2] R. E. Collin and F. J. Zucker, Eds., *Antennas Theory—Part II*. New York: McGraw-Hill, 1969.
[3] J. Jacobsen, "Analytical, numerical, and experimental investigation of guided waves on a periodically strip-loaded dielectric slab," *IEEE Trans. Antennas Propagat.*, vol. AP-18, pp. 379–388, May 1970.
[4] S. T. Peng, T. Tamir, and H. Bertoni, "Theory of periodic dielectric waveguides," *IEEE Trans. Microwave Theory Tech.*, vol. MTT-23, pp. 123–133, Jan. 1975.
[5] K. Ogusu, "Propagation properties of a planar dielectric waveguide with periodic metallic strips," *IEEE Trans. Microwave Theory Tech.*, vol. MTT-29, pp. 16–21, Jan. 1981.
[6] M. Matsumoto, M. Tsutsumi, and N. Kumagai, "Radiation characteristics of a dielectric slab waveguide with periodic metallic strips," *IEEE Trans. Microwave Theory Tech.*, vol. MTT-35, pp. 39–1042, Nov. 1987.
[7] A. Sommerfeld, *Optics: Lectures on Theoretical Physics—Vol. IV*. New York: Academic, 1964.
[8] V. A. Manasson, L. S. Sadovnik, P. I. Shnitser, R. Mino, and L. Q. Bui, "Leaky wave antenna for W-band," presented at the *Proc. Antenna Appl. Symp.*, Monticello, Il, 1995.

The Influence of Ground-Plane Width on the Ohmic Losses of Coplanar Waveguides with Finite Lateral Ground Planes

Giovanni Ghione and Michele Goano

***Abstract*— In this paper, analytical computer-aided-design (CAD)-oriented conformal-mapping approximations are presented for the high-frequency attenuation of symmetric and asymmetric coplanar waveguides (ACPW's) with finite-extent lateral ground planes. A discussion is presented on the effect of ground-plane width on the losses, and design criteria are derived.**

***Index Terms*—Attenuation, conformal mapping, coplanar waveguides, design automation software.**

I. INTRODUCTION

Coplanar waveguides (CPW's) are currently used extensively in both microwave integrated circuits (MIC's) and electro-optic components on $LiNbO_3$ substrates. In practice, such lines always have ground planes of finite width, as shown in the insets of Figs. 1 and 2 for the symmetric CPW and the asymmetric CPW, respectively. While in the design of MIC's the choice of lateral ground width is mainly driven by layout considerations (i.e., the ground-plane width $c - b$ should be large enough to avoid coupling between neighboring lines, without unnecessarily increasing the circuit size [1]), the performance optimization of electro-optic components such as amplitude and phase modulators often requires the use of very narrow lateral ground planes, as discussed in [2], [3].

From the standpoint of the CPW performances, reducing the ground-plane width causes an increase of the line impedance [see [1] for the symmetric and [4] for the asymmetric case, which can be derived from the analysis of the asymmetric coplanar stripline (ACPS)] but also of the line losses, which can significantly exceed those of the ideal structure if ground planes are narrow. To analyze such an effect, this paper presents a new closed-form expression for the skin-effect conductor attenuation of the symmetric CPW with finite-extent lateral ground planes, while the losses of the asymmetric CPW are derived by suitably rearranging the expression valid for the ACPS [4].

The analysis technique is the conformal mapping method introduced by Owyang and Wu for the analysis of conductor losses in the symmetric CPW with infinite lateral ground planes [5], and later exploited by Ghione [4] for the loss analysis of general asymmetric CPW's and striplines. The analytical expressions derived are compared with numerical results obtained from two electromagnetic simulators (HFSS[1] and Explorer[2]) with fairly good agreement. Finally, some design criteria are derived both for the symmetric and asymmetric case.

II. ANALYSIS

Despite its well-known limitations in the low-frequency range [6], [7], the skin-effect analysis of losses in a planar transmission line

Manuscript received July 22, 1996; revised May 19, 1997.

The authors are with the Dipartimento di Elettronica, Politecnico di Torino, I-10129 Torino, Italy.

Publisher Item Identifier S 0018-9480(97)06070-5.

[1] Hewlett-Packard Company, Santa Rosa, CA, *HP 85180A High-Frequency Structure Simulator. User's Reference*, May 1992.

[2] Compact Software, Inc., Paterson, NJ, *Microwave Explorer*, Mar. 1996.